

## Article

# A DODTA–TPB-Based Potentiometric Sensor for Anionic Surfactants: A Computational Design and Environmental Application

Nada Glumac<sup>1</sup>, Lucija Vrban<sup>2</sup>, Robert Vianello<sup>2</sup> , Marija Jozanović<sup>3,\*</sup> , Maksym Fizer<sup>4,5</sup> ,  
Marija Kraševac Sakač<sup>6</sup> , Raffaele Velotta<sup>7</sup> , Vincenzo Iannotti<sup>7,8</sup> , Bartolomeo Della Ventura<sup>7</sup> ,  
Matija Cvetnić<sup>9</sup> , Dean Marković<sup>10</sup>  and Nikola Sakač<sup>6,\*</sup> 

<sup>1</sup> Međimurske vode d.o.o., 40000 Čakovec, Croatia; nada.glumac@medjimurske-vode.hr

<sup>2</sup> Laboratory for the Computational Design and Synthesis of Functional Materials, Division of Organic Chemistry and Biochemistry, Ruder Bošković Institute, 10000 Zagreb, Croatia; lucija.vrban@irb.hr (L.V.); robert.vianello@irb.hr (R.V.)

<sup>3</sup> Department of Chemistry, University of Osijek, 31000 Osijek, Croatia

<sup>4</sup> Department of Organic Chemistry, Uzhhorod National University, 88000 Uzhhorod, Ukraine; max.fizer@uzhnu.edu.ua

<sup>5</sup> Department of Chemistry, University of Nevada, Reno, NV 89557, USA

<sup>6</sup> Faculty of Geotechnical Engineering, University of Zagreb, 42000 Varaždin, Croatia; msakac@gfv.unizg.hr

<sup>7</sup> Department of Physics “E. Pancini”, Università Di Napoli Federico II, 80126 Napoli, Italy; rvelotta@unina.it (R.V.); viannotti@unina.it (V.I.); bartolomeo.dellaventura@unina.it (B.D.V.)

<sup>8</sup> CNR–SPIN, c/o Department of Physics “E. Pancini”, Piazzale V. Tecchio 80, 80125 Naples, Italy

<sup>9</sup> Faculty of Chemical Engineering and Technology, University of Zagreb, Trg Marka Marulića 19, 10000 Zagreb, Croatia; mcvetnic@fkit.unizg.hr

<sup>10</sup> Department of Biotechnology, University of Rijeka, 51000 Rijeka, Croatia; dean.markovic@biotech.uniri.hr

\* Correspondence: mjozanovic@kemija.unios.hr (M.J.); nsakac@gfv.unizg.hr (N.S.)

## Abstract

Surfactants are used in various washing applications with potential negative environmental and health impacts. The ion-pair 1,3-dioctadecyl-1*H*-1,2,3-triazol-3-ium-tetraphenylborate (DODTA–TPB) was used to fabricate the potentiometric sensor for the quantification of anionic surfactants. The computational analysis of the DODTA<sup>+</sup>–TPB<sup>−</sup> adduct reveals a dynamic, thermodynamically favorable interaction driven primarily by hydrophobic C–H⋯π contacts and the flexibility of the C-18 chains, rather than electrostatic or π–π stacking forces. These findings, supported by the MM-PBSA, RDF, and structural analyses, align with broader trends in molecular recognition and provide a foundation for designing advanced ion-pair-based sensors. The sensor showed advanced analytical properties to anionic surfactants with low interfering effects of selected anions. The response of the SDS was investigated in the range from 8.1 × 10<sup>−8</sup> M to 1.0 × 10<sup>−2</sup> M, with a slope of −59.2 mV and a limit of detection (LOD) of 3.1 × 10<sup>−7</sup> M; and DBS was in the range of 8.1 × 10<sup>−8</sup> M to 2.5 × 10<sup>−3</sup> M with a slope of −57.5 mV and an LOD of 5.9 × 10<sup>−7</sup> M. The sensor was tested on potential interfering ions. Potentiometric titrations of technical-grade anionic surfactants had high recovery rates from 100.2 to 100.4%. The recovery test for spiked samples of surface waters was from 94.2 to 96.5%. The sensor was tested on commercial samples containing anionic surfactants, and the results were compared and showed a good agreement with the two-phase titration method.

**Keywords:** anionic surfactant; potentiometry; sensor; ion-pair; water analysis; DFT



Received: 30 June 2025

Revised: 5 August 2025

Accepted: 11 August 2025

Published: 1 September 2025

**Citation:** Glumac, N.; Vrban, L.; Vianello, R.; Jozanović, M.; Fizer, M.; Sakač, M.K.; Velotta, R.; Iannotti, V.; Della Ventura, B.; Cvetnić, M.; et al. A DODTA–TPB-Based Potentiometric Sensor for Anionic Surfactants: A Computational Design and Environmental Application. *Chemosensors* **2025**, *13*, 321. <https://doi.org/10.3390/chemosensors13090321>

**Copyright:** © 2025 by the authors.

Licensee MDPI, Basel, Switzerland.

This article is an open access article distributed under the terms and conditions of the Creative Commons Attribution (CC BY) license

(<https://creativecommons.org/licenses/by/4.0/>).

## 1. Introduction

Surfactants, or surface-active agents, are amphiphilic compounds that reduce the surface and interfacial tension between different phases (liquid–liquid, liquid–gas, or liquid–solid). They consist of a hydrophilic (water-attracting) head and a hydrophobic (water-repelling) tail, allowing them to interface between polar and non-polar substances. The main properties in physical terms are (i) the critical micelle concentration (CMC)—the concentration at which surfactants self-assemble into micelles, essential for detergency and emulsification; (ii) the surface tension reduction, which enables wetting, foaming, and emulsification; and (iii) self-assembly and micelle formation, where surfactants organize into micelles, bilayers, and vesicles, which is critical for biological membranes and drug delivery. They have a wide range of applications across different industries: detergents such as cleaning and disinfection products, pharmaceuticals and drug delivery, the food industry, the petroleum industry, cosmetics and personal care, nanotechnology and material science, etc. Among them, anionic surfactants dominate global production, making up approximately 70% of the market, with an increasing demand due to their effectiveness in home and personal care products. The expanding consumer market has led to a significant rise in surfactant consumption, with the industry valued at USD 45.57 billion in 2024 and anticipated to reach around USD 76.81 billion by 2034, expanding at a CAGR of 5.36% from 2025 to 2034 [1].

Since they are widely used, surfactants are often emitted into the environment. Classical methods for surfactant analysis are as follows: (1) The two-phase titration method [2], where the titration of an anionic surfactant with a cationic surfactant is performed in the presence of a mixed indicator, like methylene blue/dimidium bromide or tetrabromophenolphthalein ethyl ester, until a color change indicates the end-point. The color of the organic phase will change when the anionic surfactant is completely neutralized by the cationic surfactant. (2) The MBAS (Methylene Blue Active Substances) method [3,4] involves the formation of a colored complex between the anionic surfactant and the cationic dye methylene blue, which is then extracted into an organic solvent, and the blue color intensity is measured by a spectrophotometer. The presented methods are expensive and time-consuming, use toxic chemicals, and produce toxic waste; also, they require skilled personnel [5–9]. On the other hand, chemical sensors for surfactants, especially electrochemical surfactant sensors, are much simpler, cheaper, faster, and easier to operate [10–12]. Usually, the main component of the potentiometric surfactant sensors is the ion-pair, which is incorporated in the polymer (like PVC) enriched with a specific organic plasticizer [13–16]. The ion-pair usually consists of the cationic surfactant and a negatively charged anionic surfactant or some other high-molecular-weight anion, like tetraphenyl borate (TPB)—an organoboron anion consisting of a central boron atom with four phenyl groups [17]. The synthesis and selection of the ion-pair components are of the most importance to the sensing membrane preparation and potentiometric response [18,19]. The ideal ion-pair should have a low water solubility, a low level of leaching from the membrane, and high lipophilicity, and, finally, the sensing membrane itself should have a high resistance [10,20,21]. In this way, the fabricated surfactant sensors could have a high response, extended lifetime, and broad useful concentration range [22–24]. To fulfill all these requirements, new ion-pairs need to be synthesized and investigated through both experiments and chemical modeling [17,25,26].

From a computational perspective, the design and optimization of ion-pairs for potentiometric sensors rely on understanding the molecular interactions that govern their stability and functionality. Computational methods, such as molecular dynamics (MD) simulations and DFT computations, provide detailed insights into the electronic, geometric, and energetic properties of ion-pair adducts. These techniques allow researchers to probe

the dynamic behavior and conformational flexibility of ionophores in condensed phases, while binding free energy estimates provide a thermodynamic basis for assessing the feasibility and reversibility of the ion-pair formation, which are crucial for the sensor performance. By integrating computational modeling with experimental validation, researchers can predict the behavior of ion-pairs under various conditions, guiding the rational design of advanced ionophores with tailored properties for specific analytical applications.

In our recent work, we introduced a novel ion-pair, 1,3-dioctadecyl-1*H*-1,2,3-triazol-3-ium tetraphenylborate (DODTA-TPB), characterized and utilized as the active component in a PVC-based liquid membrane potentiometric sensor for cationic surfactants [27]. The present study extends this research by employing DODTA-TPB as the active molecule in a potentiometric sensor for anionic surfactants, such as sodium dodecyl sulfate (SDS) and sodium dodecyl benzenesulfonate (DBS). Through molecular dynamics (MD) simulations, molecular mechanics Poisson-Boltzmann surface area (MM-PBSA) calculations, and radial distribution function (RDF) analyses, we elucidated the structural and energetic properties of the DODTA-TPB adduct. These computational methods revealed that hydrophobic C-H $\cdots$  $\pi$  interactions and the flexibility of the C-18 alkyl chains dominate the ion-pair stability, with minimal contributions from electrostatic or  $\pi$ - $\pi$  stacking forces. These findings guided the design of the sensor by ensuring reversible binding and high lipophilicity, which is critical for the selective detection of anionic surfactants in complex aqueous environments. Compared to traditional methods like the ISO 2271 two-phase titration, which is time-consuming and relies on toxic organic solvents, the DODTA-TPB sensor offers a simpler, faster, and greener alternative, aligning with EU water quality directives (e.g., Directive 2000/60/EC) that emphasize the rapid and sustainable monitoring of pollutants like surfactants. By integrating computational modeling with experimental validation, this study establishes a robust framework for designing next-generation ion-pair-based sensors with an optimized performance for environmental and industrial applications.

## 2. Materials and Methods

### 2.1. Chemicals and Materials

Chemicals for organic synthesis were 1,2,3-1*H*-triazole, 1-bromooctadecane, NaHCO<sub>3</sub> (Sigma Aldrich, Darmstadt, Germany), and sodium tetraphenylborate (TPB) (Fluka, Buchs, Switzerland). To prepare the sensing membrane, following chemicals were used: o-nitrophenyloctylether (o-NPOE) (Merck, Darmstadt, Germany), high-molecular-weight PVC (Sigma-Aldrich, Hamburg, Germany), and tetrahydrofuran (THF) (Merck, Darmstadt, Germany). Chemicals for potentiometric measurements were anionic surfactants with analytical grade: sodium dodecylsulfate (SDS) and sodium dodecylbenzenesulfonate (DBS) (all from Fluka, Buchs, Switzerland); and anionic surfactants with technical grade were SDS, DBS, and lauryl ether sulfate (LES) (all from Fluka, Buchs, Switzerland). Analytical-grade chemicals for interference measurements were all from Kemika, Zagreb, Croatia. Potentiometric titrations were carried out with titrant 1,3-didecyl-2-methylimidazolium chloride (DMIC) (Merck, Munich, Germany). Anionic surfactant vial test Hach Anionic Surfactants TNTplus Vial Test was purchased from Hach Lange, Berlin, Germany.

Commercial samples were purchased in the local stores. Environmental samples were sampled (500 mL) in spring 2025 at the four locations in north-west Croatia. A lake water sample was taken at Lake Motičnjak, one sample was taken at the hydro accumulation Drava, and two samples of river water were taken at the rivers Mura and Drava. All environmental samples were taken to the lab on the same day and filtered with a standard syringe filter to remove impurities. Next, they were tested on anionic surfactants by a previously published method [9] and fast commercial vial test. No sample pre-treatment of processing was applied, and the samples were spiked and measured on the same day.

Surfactant SDS (50  $\mu\text{mol}$ ) was spiked in the environmental samples and titrated with cationic surfactant DMIC in corresponding concentrations.

## 2.2. Sensor Preparation

The DODA-TPB ion-pair was synthesized according to the fast and green principle procedure described in our previous publication [27]. After the ion-pair synthesis, purification, and characterization, the ion-pair was mixed with a high-molecular-weight PVC, THF, and a plasticizer *o*-NPOE, as described previously [27]. The sensing membrane was cut into small disk and inserted into the electrode body containing 3 M sodium chloride (Kemika, Zagreb, Croatia). The DODA-TPB surfactant sensor was stored in deionized water after measurements.

## 2.3. Measuring Setup

The potentiometric response measurements were carried out on dosing device Metrohm 794 Basic Titrimo interconnected with Metrohm 781 pH meter (Metrohm, Herisau, Switzerland). Potentiometric titrations were performed by titration device Metrohm 808 Titrand with Tiamo software (Metrohm, Herisau, Switzerland).

## 2.4. Computational Details

Initial structures of DODTA<sup>+</sup>, TPB<sup>-</sup>, and all model compounds were constructed using MarvinSketch (ChemAxon) [28]. Geometry optimizations were performed using density functional theory (DFT) at the B3LYP/6-31+G(d) level of theory in Gaussian 16 [29]. [REF] Frequency calculations were conducted at the same level to confirm that all optimized structures corresponded to true minima. Electrostatic potential (ESP) calculations were then performed at the HF/6-31G(d) level, and RESP (Restrained Electrostatic Potential) charges were derived for use in molecular mechanics simulations. The General AMBER Force Field (GAFF) was employed for all organic molecules. RESP charges and GAFF atom types were assigned using Antechamber [30]. The resulting input files were processed using ACPYPE to generate GROMACS-compatible topology (.top) and coordinate (.gro) files. Each system was solvated in a truncated octahedral simulation box with a minimum 6 Å buffer between the solute and the box edge, using the TIP3P water model. Counterions were added as needed to maintain charge neutrality. All molecular dynamics simulations were performed using GROMACS 2025.15. Energy minimization was first carried out using the steepest descent algorithm until the maximum force was below 1000 kJ mol<sup>-1</sup> nm<sup>-1</sup>. Covalent bonds involving hydrogen atoms were constrained using the LINCS algorithm, allowing a 2 fs integration timestep. Long-range electrostatic interactions were calculated using the particle mesh Ewald (PME) method with a 1.0 nm cutoff. Van der Waals interactions were treated with the same cutoff. Following energy minimization, the systems were equilibrated under NVT and then NPT conditions. Production simulations were performed for 300 ns in the NPT ensemble at 300 K and 1 bar, using the velocity-rescaling thermostat and the *c*-rescale barostat. Binding free energies were calculated using the Molecular Mechanics Generalized Born Surface Area (MMGBSA) method as implemented in the gmx\_MMPBSA package. Representative snapshots were extracted every 1 ns from the final 100 ns of each simulation for statistical averaging. Trajectory analyses included cluster analysis, radial distribution function (RDF) calculations, and interatomic distance measurements, all performed using standard GROMACS tools. Visual inspection and qualitative analysis of key interaction motifs were carried out using PyMOL 3.1.

### 3. Results and Discussion

#### 3.1. Computational Analysis

The computational analysis was conducted to gain deeper insight into the dynamic behavior of the DODTA<sup>+</sup> cation in an aqueous environment and to elucidate the intermolecular interactions that facilitate its adduct formation with the TPB<sup>−</sup> anion. This study particularly emphasizes the electronic, geometric, and energetic characteristics that define the DODTA–TPB adduct, employing molecular dynamics (MD) simulations, molecular mechanics Poisson–Boltzmann surface area (MM-PBSA) calculations, and radial distribution function (RDF) analyses. These methods are widely employed in the literature to study ion-pair interactions and molecular recognition processes [31].

Although the DODTA<sup>+</sup> molecule possesses a rigid triazole core, it exhibits significant flexibility due to the presence of two unconstrained lipophilic C-18 chains. This inherent molecular flexibility, in contrast to the relatively rigid TPB<sup>−</sup> anion, is clearly demonstrated in the calculated root-mean-square deviation (RMSD) analysis (Figure S1). The RMSD, a standard metric in MD simulations, quantifies the structural deviations of DODTA<sup>+</sup> over time, reflecting its ability to adopt multiple conformations in the solution. This conformational adaptability is consistent with findings in the literature on amphiphilic molecules, where long alkyl chains enhance flexibility and facilitate interactions with hydrophobic or aromatic partners [32]. As will be detailed in the following discussion, this adaptability of DODTA<sup>+</sup> is a key factor in its efficient recognition and interaction with TPB<sup>−</sup>, enabling the cation to adjust its geometry to optimize binding.

The adduct formation between DODTA<sup>+</sup> and TPB<sup>−</sup> is a thermodynamically favorable process; however, the analysis reveals that the adduct is not static and undergoes a continuous association and dissociation over the simulation time. The dynamic nature of the DODTA–TPB ion-pair is evidenced by the fluctuating B(TPB<sup>−</sup>)⋯N(DODTA<sup>+</sup>) distances observed during the simulation (Figure S2). These distances exceed 15 Å in some instances, indicating a temporary dissociation, while in approximately 66% of the sampled structures, they remain below 6 Å, suggesting close contact. This behavior aligns with studies on ion-pair dynamics in aqueous media, where weak or reversible interactions lead to a broad distribution of intermolecular distances [33]. Despite this variability, the MM-PBSA calculations indicate that the binding free energy for DODTA<sup>+</sup> and TPB<sup>−</sup> is exergonic, with a  $\Delta G_{\text{BIND}}$  value of  $-23.4 \text{ kcal mol}^{-1}$ . This negative binding energy confirms the feasibility of the interaction and suggests a delicate balance between adduct stability and reversibility. In the context of sensor applications, this balance is crucial, as it ensures the formation of a stable ion-pair while permitting a reversible dissociation, which is essential for the detection and exchange of other anionic analytes in the solution.

The structural analysis of the representative DODTA–TPB adduct (Figure 1) identifies two predominant types of stabilizing interactions: (1) the  $\pi$ – $\pi$  stacking between the triazole moiety of DODTA<sup>+</sup> and a phenyl ring of TPB<sup>−</sup>, and (2) multiple C–H⋯ $\pi$  interactions between the flexible C-18 chains of DODTA<sup>+</sup> and additional phenyl rings in TPB<sup>−</sup>. These interactions are consistent with those reported for aromatic systems in aqueous environments, where  $\pi$ – $\pi$  stacking and C–H⋯ $\pi$  contacts often drive molecular recognition [34]. The boron–nitrogen separation, measured from the central unsubstituted triazole nitrogen in DODTA<sup>+</sup> of 5.2 Å in the representative structure, closely aligns with the radial distribution function (RDF) analysis, which shows a peak at 5.4 Å (Figure 1). The RDF analysis quantifies the probability of finding the boron atom of TPB<sup>−</sup> at a given distance from the representative nitrogen atom of DODTA<sup>+</sup>, confirming the dynamic yet stable nature of the adduct. This consistency supports the validity of the proposed representative structure and highlights the key molecular interactions responsible for the stability and functionality of the DODTA–TPB ion-pair.

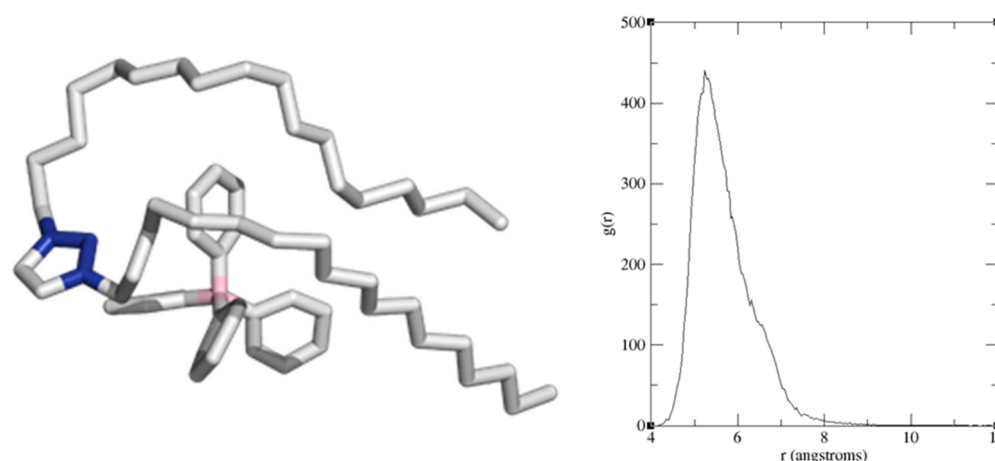


**Figure 1.** The representative structure of the DODTA–TPB adduct in the aqueous solution (**left**; hydrogen atoms omitted for clarity) as elucidated from the 300 ns molecular dynamics simulations. The corresponding radial distribution function (RDF) graph (**right**) shows the distribution of N(DODTA<sup>+</sup>)...B(TPB<sup>−</sup>) distances involving the central unsubstituted triazole nitrogen in the cation, with a peak at 5.4 Å, indicating the preferred intermolecular separation in the adduct.

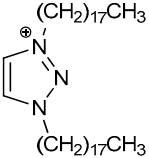
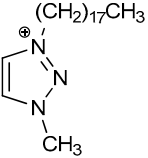
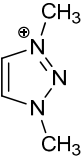
The close proximity between the boron and nitrogen atoms in the DODTA–TPB ion-pair may initially suggest that electrostatic attraction is the dominant force driving the binding between the opposite charges of DODTA<sup>+</sup> and TPB<sup>−</sup>. However, this hypothesis can be ruled out based on a thorough analysis of atomic charge distributions before and after the adduct formation (Figure S3). The findings indicate that, prior to binding, the triazole unit in DODTA<sup>+</sup> only accommodates approximately one-third of the excess positive charge (0.28 |e|), while the remaining charge is distributed within the C-18 alkyl chains. Interestingly, this distribution remains unchanged after the adduct is formed, which suggests that electrostatic interactions do not play a predominant role in stabilizing the adduct. In fact, upon the formation of the DODTA–TPB adduct, only 1% of the total charge density is exchanged between the two components. This is evident from the sum of the atomic charges on DODTA<sup>+</sup> and TPB<sup>−</sup> within the adduct, which have values of +1.01 |e| and −0.99 |e|, respectively. These results conclusively eliminate electrostatic interactions as a major contributor to the stability of the adduct, suggesting that hydrophobic and dispersion forces dominate the interaction.

Furthermore, we investigated the extent of  $\pi\cdots\pi$  stacking interactions among the components by analyzing the distances between the center of the mass of the triazole ring in DODTA<sup>+</sup> and the phenyl groups in TPB<sup>−</sup>. Using the commonly accepted 4 Å threshold for  $\pi\cdots\pi$  interactions [25], we observed that such interactions only occur in 11% of the structures sampled during the molecular dynamics simulations. These relatively low frequencies suggest that  $\pi\cdots\pi$  interactions between formally charged groups only marginally contribute to the overall adduct formation, further highlighting their limited role in stabilizing the adduct.

In an effort to better understand the contribution of the C–H $\cdots\pi$  interactions, we examined a series of model cationic components, replacing one or both of the C-18 alkyl chains in DODTA<sup>+</sup> with smaller methyl groups (Table 1). This modification allows us to assess the impact of the alkyl chains on the binding affinity. The results revealed that when one C-18 chain was substituted with a methyl group, the binding affinity decreased almost by half ( $\Delta G_{\text{BIND}} = -14.9 \text{ kcal mol}^{-1}$ ). Furthermore, when both C-18 chains were consistently replaced with methyl groups, the binding affinity showed an even more substantial 79% reduction ( $\Delta G_{\text{BIND}} = -5.0 \text{ kcal mol}^{-1}$ ). These findings underscore the critical role of the long alkyl chains in facilitating the binding of TPB<sup>−</sup>, as their presence significantly enhances

the affinity of the cationic DODTA<sup>+</sup> for TPB<sup>-</sup>. This observation is further supported by simulations involving a simple alkane, C<sub>36</sub>H<sub>74</sub>, which is composed of two alkyl chains of equivalent lengths to those in DODTA<sup>+</sup>. Despite being formally uncharged, C<sub>36</sub>H<sub>74</sub> demonstrated a binding affinity for TPB<sup>-</sup> that almost surpassed that of the model cationic triazoles,  $\Delta G_{\text{BIND}} = -12.0 \text{ kcal mol}^{-1}$  (Table 1), thus retaining approximately 51% of the full DODTA<sup>+</sup> affinity. This suggests that the hydrophobic interactions provided by the alkyl chains, along with their flexibility, play a dominant role in recognizing and binding TPB<sup>-</sup> in the solution.

**Table 1.** MM-PBSA calculated binding affinities ( $\Delta G_{\text{BIND}}$ , in kcal mol<sup>-1</sup>) between the TPB<sup>-</sup> anion and selected cations following the molecular dynamics simulations in water.

Cation Component				CH <sub>3</sub> (CH <sub>2</sub> ) <sub>34</sub> CH <sub>3</sub>
$\Delta G_{\text{BIND}}$	-23.4	-14.9	-5.0	-12.0

The dominance of the hydrophobic interactions and the flexibility of the C-18 chains have significant implications for designing potentiometric sensors based on ionophores like DODTA<sup>+</sup>. The reversible nature of the DODTA-TPB adduct, balanced by a favorable  $\Delta G_{\text{BIND}}$  value, aligns with the requirements for selective ion detection, where stability and exchangeability are key [13]. The limited contribution of electrostatics suggests that future designs could prioritize hydrophobic motifs to enhance the binding affinity, while maintaining a minimal charge dependence to improve selectivity in complex aqueous environments. These insights build on the existing literature, where hydrophobic cavities and flexible alkyl chains are engineered into ionophores to optimize the performance [35].

### 3.2. Potentiometric Sensor Characterization

The first step in the DODTA-TPB surfactant sensor characterization was to observe the response characteristics of the sensor toward selected anionic surfactants. The sensor response mechanism corresponds to the modified Nernstian equation (Equation (1)):

$$E = E_0 - S \log a_{AS^-} \quad (1)$$

where  $E$  is an electrode potential,  $E_0$  is a standard electrode potential,  $S$  is the slope of the electrode, and  $a_{AS^-}$  is the activity of the investigated surfactant anion.

SDS and DBS were used as model molecules to observe the response characteristics of the DODTA-TPB surfactant sensor to anionic surfactants. The response measurements were carried out in deionized water. The response characteristics of SDS were investigated in the range from  $8.1 \times 10^{-8} \text{ M}$  to  $1.0 \times 10^{-2} \text{ M}$ , while the response characteristics of DBS were investigated in the range from  $8.1 \times 10^{-8} \text{ M}$  to  $2.5 \times 10^{-3} \text{ M}$  (Figure 2). The potentiometric response for SDS showed a high linear range from  $4.1 \times 10^{-7}$  to  $5.1 \times 10^{-3} \text{ M}$ , with a slope value of  $-59.2 \pm 0.4 \text{ mV/decade}$  of activity and calculated limit of detection (LOD) of  $3.1 \times 10^{-7} \text{ M}$ . The potentiometric response for DBS had a linear range from  $8.1 \times 10^{-7}$  to  $6.1 \times 10^{-4} \text{ M}$ , with a slope value of  $-57.5 \pm 0.5 \text{ mV/decade}$  of activity and a  $5.9 \times 10^{-7} \text{ M}$  LOD. Detection limits were estimated according to the IUPAC recommendations [36]. The sensor showed high stability with a signal drift of 3 mV/hour.

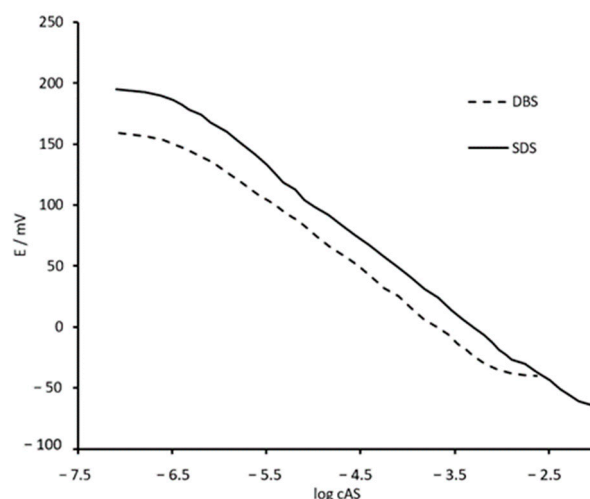


**Figure 2.** Potentiometric response curves of the DODTA-TPB surfactant sensor to anionic surfactants SDS and DBS in deionized water. The curves were rearranged vertically for clarity.

The comparison with previously published response characteristics of ion-pairs containing TPB as a counter ion showed a good agreement with new DODTA-TPB ion-pair sensing properties to the anionic surfactants DBS and SDS in terms of the linear response range, slope per decade of activity, and LOD (Table 2).

**Table 2.** Response characteristics of potentiometric surfactants sensors based on different ion-pairs containing anionic TPB counter ion.

AS *	Sensor Characteristic	Ion-Pair				
		New DODTA-TPB	DMIC-TPB [37]	DODI-TPB [25]	DHBI-TPB [38]	DDA-TPB [39]
DBS	LOD (M)	$5.9 \times 10^{-7}$	$6.0 \times 10^{-7}$	$7.1 \times 10^{-7}$	$6.1 \times 10^{-7}$	$2.0 \times 10^{-7}$
	Linear response range (M)	$8.1 \times 10^{-7}$ – $6.1 \times 10^{-4}$	$8 \times 10^{-7}$ – $6 \times 10^{-4}$	$6.3 \times 10^{-7}$ – $3.2 \times 10^{-4}$	$8.9 \times 10^{-7}$ – $4.1 \times 10^{-3}$	$2.5 \times 10^{-7}$ – $1.2 \times 10^{-3}$
	Slope (mV/decade of activity)	−57.5	−57.8	−59.3	−58.4	−55.3
SDS	LOD (M)	$3.1 \times 10^{-7}$	$3.2 \times 10^{-7}$	$6.8 \times 10^{-7}$	$3.2 \times 10^{-7}$	$2.5 \times 10^{-7}$
	Linear response range (M)	$4.1 \times 10^{-7}$ – $5.1 \times 10^{-3}$	$4.0 \times 10^{-7}$ – $5 \times 10^{-3}$	$5.9 \times 10^{-7}$ – $4.1 \times 10^{-3}$	$4.6 \times 10^{-7}$ – $5.1 \times 10^{-3}$	$3.2 \times 10^{-7}$ – $4.6 \times 10^{-3}$
	Slope (mV/decade of activity)	−59.2	−59.3	−58.3	−60.1	−58.5

\* Anionic Surfactant.

### 3.3. Interference Study

To observe the influence of potential interfering ions, a series of anions were prepared (Table 3). The concentration of the interfering ion solution was 0.01 M, for each investigated anion. SDS was incrementally added to the interfering ion solution and the DODTA-TPB surfactant sensor potentiometric response was measured. To calculate the interfering influence on potentiometric response, a fixed interference method was used [40]. For all selected anions, the logarithm of the selectivity coefficient was calculated. The DODTA-TPB surfactant sensor showed a high stability and a low influence of investigated interfering anions.

Next, the influence of the pH on the DODTA-TPB surfactant sensor potentiometric response on SDS was investigated. The sensor showed a high stability in the range from pH 3 to 10. Small signal deviations were observed at pH 2 and from pH 11, but still there was no significant influence on the response signal.

**Table 3.** The calculated selectivity coefficient (logarithm) for selected anions (0.01 M) measured with the DODTA-TPB surfactant sensor for the anionic surfactant SDS.

Interfering Anions	$\log K_{An_i}^{pot}$
Acetate	−3.72
Benzoat	−3.84
Bromide	−3.21
Borate	−2.98
Chloride	−3.83
Carbonate	−4.14
Dihydrogenphosphate	−4.01
EDTA	−3.84
Fluoride	−3.68
Hydrogen carbonate	−4.02
Hydrogen sulfate	−3.86
Nitrate	−3.93
Sulfate	−4.62

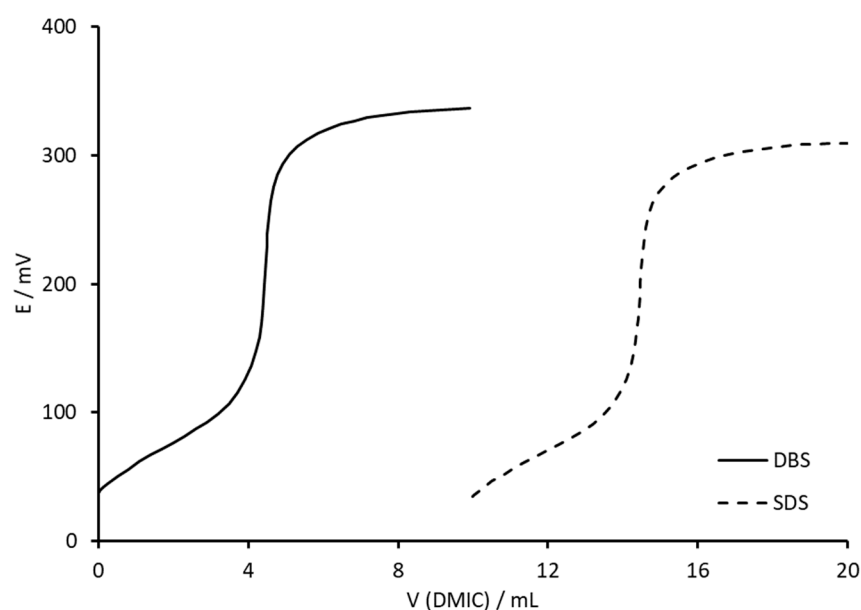
### 3.4. Potentiometric Titrations of Model and Environmental Samples

For the titration of anionic surfactants SDS ( $4 \times 10^{-3}$  M) and DBS ( $4 \times 10^{-3}$  M), the cationic surfactant DMIC was used. The chemical reaction is as follows (Equation (2)):



The  $An_{AS}^-$  represents the anionic surfactant (analyte, SDS, or DBS), the  $Cat_{CS}^+$  represents the cationic surfactant (titrant, DMIC), and the  $An_{AS}Cat_{CS}$  is the low solubility complex, usually manifesting as a white precipitate.

Potentiometric titration curves for the titration of SDS ( $4 \times 10^{-3}$  M) and DBS ( $4 \times 10^{-3}$  M) with DMIC cationic surfactants ( $4 \times 10^{-3}$  M) used as a titrant are presented in Figure 3. The DODTA-TPB surfactant sensor was used as an end-point indicator. The titration curves for the model samples of SDS and DBS had defined and sharp inflection points with a high potential signal change (Figure 3). The end-point could be easily detected.

**Figure 3.** Potentiometric titrations of model samples containing DBS ( $4 \times 10^{-3}$  M, full line) and SDS ( $4 \times 10^{-3}$  M, dashed line) with DMIC cationic surfactants, DMIC ( $4 \times 10^{-3}$  M), and the DODTA-TPB surfactant sensor as the end-point detector. The titration curves were rearranged horizontally for clarity.

To observe the behavior of the DODTA-TPB surfactant sensor in solutions of the technical-grade anionic surfactant, a series of three anionic surfactants (SDS, DBS, and lauryl ether sulfate (LES)) were titrated, with DMIC ( $4 \times 10^{-3}$  M) as a titrant. A fixed amount of the technical-grade anionic surfactant was added to the deionized water and titrated by the DODTA-TPB surfactant sensor as an end-point indicator. The titration curves were sigmoidal, with well-defined inflection points. The overall signal change ( $\Delta E$ ) was 301.1 mV for the DBS titration curve and 276.2 mV for the SDS titration curve. Calculated recoveries were from 100.2 to 100.4%, respectively (Table 4).

**Table 4.** Potentiometric titrations of three technical-grade anionic surfactants with DMIC ( $4 \times 10^{-3}$  M) as a titrant and the DODTA-TPB surfactant sensor as an end-point indicator, with mean values at  $\pm 95\%$  confidence limits.

Technical-Grade Anionic Surfactant	$w$ (Surfactant) */%	$n$ (Added)/ $\mu\text{mol}$	$n$ (Found) **/ $\mu\text{mol}$	Recovery/%
SDS	$91.28 \pm 0.31$	50	$50.21 \pm 0.04$	100.4
DBS	$47.61 \pm 0.25$	50	$50.13 \pm 0.09$	100.2
LES	$28.74 \pm 0.12$	50	$50.11 \pm 0.05$	100.2

\* Average of 5 measurements. \*\* Average of 5 measurements.

After testing the DODTA-TPB surfactant sensor on model solutions and technical-grade anionic surfactants, six samples of commercial products with declared anionic surfactant contents were used to qualify the amount of anionic surfactants in the samples. Powdered, liquid/gel, and handwashing detergents were purchased from the local store. DMIC (in varying concentrations) was used as a titrant, and the DODTA-TPB surfactant sensor was used as an end-point indicator (Table 5). The titration curves were well defined and sigmoidal, and the end-point could be easily calculated. Calculated values for powdered detergents were 5.83 and 6.74% of anionic surfactants, for handwashing detergents they were 13.85 and 16.41%, and for the liquid/gel detergents they were 2.57 and 2.73% of anionic surfactants. The calculated amounts of anionic surfactants were in agreement with our previous measurements [25]. For the comparison, a two-phase method [2] was used on the same samples. The calculated amounts were in good agreement with the DODTA-TPB sensor.

**Table 5.** Results for the potentiometric titration of commercial products containing anionic surfactants by the DODTA-TPB surfactant sensor compared with a two-phase titration method. DMIC was used as a titrant.

	Commercial Detergents	$w$ (ANIONIC SURFACTANT)/%	
		DODTA-TPB	Two-Phase Titration *
Powdered	sample 1	$5.83 \pm 0.21$	5.91
	sample 2	$6.74 \pm 0.13$	7.01
Handwashing	sample 3	$13.85 \pm 0.56$	13.69
	sample 4	$16.41 \pm 0.06$	16.08
Liquid/gel	sample 5	$2.57 \pm 0.06$	2.66
	sample 6	$2.72 \pm 0.19$	2.76

\* [2].

The DODTA-TPB surfactant sensor was used as an end-point indicator in the potentiometric titrations of environmental water samples from the following locations in north-west Croatia: one sample of lake water (lake Motičnjak); one sample of hydroaccumulation Drava; and two samples of river water (rivers Mura and Drava). pH values were measured

in all the samples and were in the range from 7.7 to 8.5. All environmental samples were tested on anionic surfactants by a previously published method [37] and fast commercial vial test and showed no anionic surfactants presence in the samples. The anionic surfactant SDS (50  $\mu\text{mol}$ ) was spiked in the environmental samples and titrated with DMIC. The recovery results are shown in Table 6. SDS was successfully quantified in all environmental samples, which is a promising result since no matrix interfering effect was observed, and recoveries were in the range from 94.2 to 96.5%.

**Table 6.** Recoveries for the potentiometric titration of spiked SDS (50  $\mu\text{mol}$ ) in environmental samples by the DODTA-TPB surfactant sensor as an end-point indicator. DMIC was used as a titrant.

Sampling Place	Vial Test	Added SDS	Recovery%
River Drava	No A.S. *	50 $\mu\text{mol}$	96.5%
River Mura	No A.S.	50 $\mu\text{mol}$	95.8%
Lake Motičnjak	No A.S.	50 $\mu\text{mol}$	94.2%
Hydro accumulation Drava	No A.S.	50 $\mu\text{mol}$	94.5%

\* A.S.—anionic surfactant.

#### 4. Conclusions

The development of a DODTA-TPB-based potentiometric sensor represents a significant advancement in the detection of anionic surfactants, offering a sensitive, selective, and environmentally friendly alternative to traditional methods. The computational analysis, utilizing molecular dynamics simulations, MM-PBSA calculations, and RDF analyses, elucidated the dynamic and thermodynamically favorable interactions between the DODTA<sup>+</sup> cation and TPB<sup>−</sup> anion, primarily driven by hydrophobic C–H $\cdots\pi$  contacts and the flexibility of the C-18 alkyl chains. These findings highlight the limited role of electrostatic and  $\pi$ – $\pi$  stacking interactions, emphasizing the importance of hydrophobic forces in stabilizing the ion-pair adduct, which is critical for its functionality in sensor applications, thus ensuring stable yet reversible binding with target analytes. The sensor demonstrated excellent near-Nernstian responses for SDS and DBS, with low detection limits and a broad linear response range, making it suitable for both trace-level and high-concentration measurements. Its reliability was further confirmed through the minimal interference from common anions and the consistent performance across a wide pH range.

Practical applications highlighted the sensor's accuracy, with near-quantitative recoveries in technical-grade surfactants and a strong agreement with standard methods in commercial product testing. The environmental analyses of spiked water samples yielded high recovery rates, proving its effectiveness in real water samples. The sensor's simplicity, cost-efficiency, and reduced need for toxic reagents align with the growing demand for sustainable analytical tools. Using the computational insights and practical potentiometric measurements, this work provides a blueprint for designing advanced ion-selective sensors. Future research could expand its use to other surfactant classes or integrate it into portable systems for on-site monitoring, further enhancing its impact on environmental and industrial applications.

**Supplementary Materials:** The following supporting information can be downloaded at <https://www.mdpi.com/article/10.3390/chemosensors13090321/s1>: Figure S1: RMSD graphs from the molecular dynamics simulation of the DODTA<sup>+</sup> cation (in black) and the TPB<sup>−</sup> anion (in red) in aqueous solution, showing significantly higher flexibility of the former; Figure S2: Evolution of the distance between the boron atom in TPB<sup>−</sup> and the nitrogen atoms in DODTA<sup>+</sup> during the molecular dynamics simulation, indicating that the DODTA–TPB adduct formation is reversible and in equilibrium with the dissociated components; Figure S3: Charge distribution within the DODTA<sup>+</sup> cation and the TPB<sup>−</sup> anion, either isolated or within the elucidated representative structure of the DODTA–TPB adduct,

as obtained from the NBO analysis at the (SMD)/M06–2X/6–31+G(d) level of theory in water. The specific set of atoms considered for the analysis is denoted by color (red for the cation, blue for the anion) and includes the attached hydrogen atoms. The results reveal that only 1% of the charge density is transferred between the overall components following DODTA–TPB adduct formation.

**Author Contributions:** Conceptualization, R.V. (Robert Vianello), L.V., N.G., M.J. and N.S.; methodology, M.J., N.S., N.G., R.V. (Robert Vianello), L.V. and M.F.; software, R.V. (Robert Vianello), L.V. and M.F.; validation, N.S., M.J. and N.G.; formal analysis, N.G., R.V. (Robert Vianello), L.V., M.F., M.C., D.M. and M.K.S.; investigation, N.G., M.K.S., N.S. and M.J.; resources, N.G., M.J., N.S., D.M., R.V. (Raffaele Velotta), B.D.V. and V.I.; data curation, N.G., R.V. (Raffaele Velotta), B.D.V., V.I. and M.C.; writing—original draft preparation, R.V. (Robert Vianello), L.V., N.G., M.J. and N.S.; writing—review and editing, N.G., M.J., N.S., R.V. (Robert Vianello), M.F., L.V., R.V. (Raffaele Velotta) and V.I.; visualization, N.G., M.K.S., N.S. and M.J.; supervision, N.S. and M.J.; project administration, N.G., M.K.S., N.S. and M.J.; funding acquisition, M.J., N.S., R.V. (Raffaele Velotta), B.D.V., V.I. and D.M. All authors have read and agreed to the published version of the manuscript.

**Funding:** Part of this work was supported by the Croatian Science Foundation [grant number IP-2020-02-8090].

**Institutional Review Board Statement:** Not applicable.

**Informed Consent Statement:** Not applicable.

**Data Availability Statement:** The data presented in this study are available on request.

**Acknowledgments:** L.V. and R. Vianello thank the Zagreb University Computing Centre (SRCE) for granting computational resources on the SUPEK supercomputer.

**Conflicts of Interest:** Nada Glumac was employed by the company Međimurske vode d.o.o. The remaining authors declare that the research was conducted in the absence of any commercial or financial relationships that could be construed as a potential conflict of interest.

## References

1. Presedence Research Surfactants Market Size, Share and Trends 2025 to 2034. Available online: <https://www.precedenceresearch.com/surfactants-market#:~:text=Report%20Code%203A%201728-,Surfactants%20Market%20Size%20and%20Forecast%2025%20to%202034,5.36%25%20from%202025%20to%202034> (accessed on 10 May 2025).
2. ISO 2271:1989; Surface Active Agents, Detergents, Determination of Anionic-Active Matter by Manual or Mechanical Direct Two-phase Titration Procedure. ISO: Geneva, Switzerland, 1989.
3. ISO 7875-1:1996; Water Quality-Determination of Surfactant-Part 1: Determination of Anionic Surfactants by Measurement of the Methylene Blue Index (MBAS). ISO: Geneva, Switzerland, 1996. Available online: <https://www.iso.org/standard/24784.html> (accessed on 7 August 2018).
4. Wyrwas, B.; Zgoła-Grzeškowiak, A. Continuous flow methylene blue active substances method for the determination of anionic surfactants in river water and biodegradation test samples. *J. Surfactants Deterg.* **2014**, *17*, 191–198. [[CrossRef](#)] [[PubMed](#)]
5. Yoon, J.H.; Shin, Y.G.; Kirkham, M.B.; Jeong, S.S.; Lee, J.G.; Kim, H.S.; Yang, J.E. A Simplified Method for Anionic Surfactant Analysis in Water Using a New Solvent. *Toxics* **2022**, *10*, 162. [[CrossRef](#)] [[PubMed](#)]
6. Yoon, J.H.; Shin, Y.G.; Kim, H.S.; Kirkham, M.B.; Yang, J.E. Screening of a Novel Solvent for Optimum Extraction of Anionic Surfactants in Water. *Toxics* **2022**, *10*, 1–13. [[CrossRef](#)] [[PubMed](#)]
7. Ródenas-Torrallba, E.; Reis, B.F.; Morales-Rubio, Á.; De La Guardia, M. An environmentally friendly multicommutated alternative to the reference method for anionic surfactant determination in water. *Talanta* **2005**, *66*, 591–599. [[CrossRef](#)]
8. Lengyel, J.; Krtíl, J. Radiometric determination of anionic surfactants by two-phase titration method with the use of 131I-Rose Bengal as indicator. *J. Radioanal. Nucl. Chem. Lett.* **1986**, *103*, 51–61. [[CrossRef](#)]
9. Miller, C.; Bageri, B.S.; Zeng, T.; Patil, S.; Mohanty, K.K. Modified Two-Phase Titration Methods to Quantify Surfactant Concentrations in Chemical-Enhanced Oil Recovery Applications. *J. Surfactants Deterg.* **2020**, *23*, 1159–1167. [[CrossRef](#)]
10. Zdrachek, E.; Bakker, E. Potentiometric Sensing. *Anal. Chem.* **2021**, *93*, 72–102. [[CrossRef](#)]
11. Kovács, B.; Csóka, B.; Nagy, G.; Ivaska, A. All-solid-state surfactant sensing electrode using conductive polymer as internal electric contact. *Anal. Chim. Acta* **2001**, *437*, 67–76. [[CrossRef](#)]
12. Khedr, A.M.; Abu Shawish, H.M.; Gaber, M.; Abed Almonem, K.I. Potentiometric Determination of Alkyl Dimethyl Hydroxyethyl Ammonium Surfactant by a New Chemically Modified Carbon Past Electrode. *J. Surfactants Deterg.* **2014**, *17*, 183–190. [[CrossRef](#)]

13. Bakker, E.; Pretsch, E.; Bühlmann, P. Selectivity of Potentiometric Ion Sensors. *Anal. Chem.* **2000**, *72*, 1127–1133. [[CrossRef](#)]
14. Mihali, C.; Vaum, N. Use of Plasticizers for Electrochemical Sensors. In *Recent Advances in Plasticizers*; InTech: London, UK, 2012.
15. Mikhelson, K.N.; Peshkova, M.A. Advances and trends in ionophore-based chemical sensors. *Russ. Chem. Rev.* **2015**, *84*, 555–578. [[CrossRef](#)]
16. Kulapina, E.G.; Ovchinskii, V.A. New modified electrodes for the separate determination of anionic surfactants. *J. Anal. Chem.* **2000**, *55*, 169–174. [[CrossRef](#)]
17. Sakač, N.; Madunić-Čačić, D.; Marković, D.; Ventura, B.D.; Velotta, R.; Ptiček Siročić, A.; Matasović, B.; Sermek, N.; Đurin, B.; Šarkanj, B.; et al. The 1,3-Dioctadecyl-1H-imidazol-3-ium Based Potentiometric Surfactant Sensor for Detecting Cationic Surfactants in Commercial Products. *Sensors* **2022**, *22*, 9141. [[CrossRef](#)]
18. Vladimirova, N.; Puchkova, E.; Dar'in, D.; Turanov, A.; Babain, V.; Kirsanov, D. Predicting the Potentiometric Sensitivity of Membrane Sensors Based on Modified Diphenylphosphoryl Acetamide Ionophores with QSPR Modeling. *Membranes* **2022**, *12*, 953. [[CrossRef](#)] [[PubMed](#)]
19. Turyshev, E.S.; Kopytin, A.V.; Zhizhin, K.Y.; Kubasov, A.S.; Shpigun, L.K.; Kuznetsov, N.T. Potentiometric quantitation of general local anesthetics with a new highly sensitive membrane sensor. *Talanta* **2022**, *241*, 123239. [[CrossRef](#)]
20. Fizer, O.; Fizer, M.; Sidey, V.; Studenyak, Y. Predicting the end point potential break values: A case of potentiometric titration of lipophilic anions with cetylpyridinium chloride. *Microchem. J.* **2021**, *160*, 105758. [[CrossRef](#)]
21. Bakker, E.; Bühlmann, P.; Pretsch, E. Carrier-Based Ion-Selective Electrodes and Bulk Optodes. 1. General Characteristics. *Chem. Rev.* **1997**, *97*, 3083–3132. [[CrossRef](#)]
22. Kumar, V.; Suri, R.; Mittal, S. Review on new ionophore species for membrane ion selective electrodes. *J. Iran. Chem. Soc.* **2023**, *20*, 509–540. [[CrossRef](#)]
23. Cuartero, M.; Más-Montoya, M.; Soledad García, M.; Curiel, D.; Ortuño, J.A. New carbazolo[1,2-a]carbazole derivative as ionophore for anion-selective electrodes: Remarkable recognition towards dicarboxylate anions. *Talanta* **2014**, *123*, 200–206. [[CrossRef](#)]
24. Krivačić, S.; Speck, A.; Kassal, P.; Bakker, E. Towards mass-production of ion-selective electrodes by spotting: Optimization of membrane composition and real-time tracking of membrane drying. *Sens. Actuators B Chem.* **2025**, *423*, 136759. [[CrossRef](#)]
25. Sakač, N.; Madunić-Čačić, D.; Marković, D.; Hok, L.; Vianello, R.; Vrček, V.; Šarkanj, B.; Đurin, B.; Della Ventura, B.; Velotta, R.; et al. Potentiometric Surfactant Sensor for Anionic Surfactants Based on 1,3-dioctadecyl-1H-imidazol-3-ium tetraphenylborate. *Chemosensors* **2022**, *10*, 523. [[CrossRef](#)]
26. Abd El-Rahman, M.K.; Zaazaa, H.E.; Eldin, N.B.; Moustafa, A.A. Just-Dip-It (Potentiometric Ion-Selective Electrode): An Innovative Way of Greening Analytical Chemistry. *ACS Sustain. Chem. Eng.* **2016**, *4*, 3122–3132. [[CrossRef](#)]
27. Glumac, N.; Fizer, M.; Sakač, N.; Marković, D.; Vrban, L.; Vianello, R.; Šarkanj, B.; Sakač, M.K.; Jozanović, M. Study of a 1,3-dioctadecyl-1H-1,2,3-triazol-3-ium cation for potentiometric surfactants sensing applications. *J. Mol. Liq.* **2025**, *432*, 127831. [[CrossRef](#)]
28. Cherinka, B.; Andrews, B.H.; Sánchez-Gallego, J.; Brownstein, J.; Argudo-Fernández, M.; Blanton, M.; Bundy, K.; Jones, A.; Masters, K.; Law, D.R.; et al. Marvin: A Tool Kit for Streamlined Access and Visualization of the SDSS-IV MaNGA Data Set. *Astron. J.* **2019**, *158*, 74. [[CrossRef](#)]
29. Frisch, M.J.; Trucks, G.W.; Schlegel, H.B.; Scuseria, G.E.; Robb, M.A.; Cheeseman, J.R.; Scalmani, G.; Barone, V.; Petersson, G.A.; Nakatsuji, H.; et al. *G16\_C01 2016, Gaussian 16, Revision C.01*; Gaussian Inc.: Wallin, UK, 2016.
30. Wang, J.; Wang, W.; Kollman, P.A.; Case, D.A. Automatic atom type and bond type perception in molecular mechanical calculations. *J. Mol. Graph. Model.* **2006**, *25*, 247–260. [[CrossRef](#)] [[PubMed](#)]
31. Genheden, S.; Ryde, U. The MM/PBSA and MM/GBSA methods to estimate ligand-binding affinities. *Expert Opin. Drug Discov.* **2015**, *10*, 449–461. [[CrossRef](#)]
32. Israelachvili, J.N. *Intermolecular and Surface Forces*; Elsevier: Amsterdam, The Netherlands, 2011; ISBN 9780123751829.
33. Marcus, Y.; Hefter, G. Ion Pairing. *Chem. Rev.* **2006**, *106*, 4585–4621. [[CrossRef](#)] [[PubMed](#)]
34. Meyer, E.A.; Castellano, R.K.; Diederich, F. Interactions with Aromatic Rings in Chemical and Biological Recognition. *Angew. Chem. Int. Ed.* **2003**, *42*, 1210–1250. [[CrossRef](#)] [[PubMed](#)]
35. Bühlmann, P.; Chen, L.D. Ion-Selective Electrodes With Ionophore-Doped Sensing Membranes. In *Supramolecular Chemistry*; John Wiley and Sons: Hoboken, NJ, USA, 2012.
36. Guilbault, G.G.; Durst, R.A.; Frant, M.S.; Freiser, H.; Hansen, E.H.; Light, T.S.; Pungor, E.; Rechnitz, G.; Rice, N.M.; Rohm, T.J.; et al. Recommendations for nomenclature of ion-selective electrodes. *Pure Appl. Chem.* **1976**, *48*, 127–132. [[CrossRef](#)]
37. Madunić-Čačić, D.; Sak-Bosnar, M.; Samardžić, M.; Grabarić, Z. Determination of anionic surfactants in industrial effluents using a new highly sensitive surfactant-selective sensor. *Sens. Lett.* **2009**, *7*, 50–56. [[CrossRef](#)]
38. Sakač, N.; Madunić-Čačić, D.; Marković, D.; Hok, L.; Vianello, R.; Šarkanj, B.; Đurin, B.; Hajdek, K.; Smoljan, B.; Milardović, S.; et al. Potentiometric Surfactant Sensor Based on 1,3-Dihexadecyl-1H-benzo[d]imidazol-3-ium for Anionic Surfactants in Detergents and Household Care Products. *Molecules* **2021**, *26*, 3627. [[CrossRef](#)] [[PubMed](#)]

39. Samardžić, M.; Galović, O.; Petrušić, S.; Sak-Bosnar, M. The Analysis of Anionic Surfactants in Effluents Using a DDA-TPB Potentiometric Sensor. *Int. J. Electrochem. Sci.* **2014**, *9*, 6166–6181. [[CrossRef](#)]
40. Buck, R.P.; Lindner, E. Recommendations for nomenclature of ion-selective electrodes (IUPAC recommendations 1994). *Pure Appl. Chem.* **1994**, *66*, 2527–2536. [[CrossRef](#)]

**Disclaimer/Publisher's Note:** The statements, opinions and data contained in all publications are solely those of the individual author(s) and contributor(s) and not of MDPI and/or the editor(s). MDPI and/or the editor(s) disclaim responsibility for any injury to people or property resulting from any ideas, methods, instructions or products referred to in the content.